



Collisions of electrons with hydrogen atoms I. Package outline and high energy code[☆]



Jakub Benda^{*}, Karel Houfek

Institute of Theoretical Physics, Faculty of Mathematics and Physics, Charles University in Prague, V Holešovičkách 2, Prague, Czech Republic

ARTICLE INFO

Article history:

Received 28 January 2014

Received in revised form

27 May 2014

Accepted 30 May 2014

Available online 10 July 2014

Keywords:

Electron–hydrogen scattering

Atomic database

Distorted-wave Born approximation

ABSTRACT

Being motivated by the applied researchers' persisting need for accurate scattering data for the collisions of electrons with hydrogen atoms, we developed a computer package – Hex – that is designed to provide trustworthy results for all basic discrete and continuous processes within non-relativistic framework. The package consists of several computational modules that implement different methods, valid for specific energy regimes. Results of the modules are kept in a common database in the unified form of low-level scattering data (partial-wave T -matrices) and accessed by an interface program which is able to produce various derived quantities like e.g. differential and integral cross sections. This article is the first one of a series of articles that are concerned with the implementation and testing of the modules. Here we give an overview of their structure and present (a) the command-line interface program hex-db that can be also easily compiled into a derived code or used as a backend for a web-page form and (b) simple illustrative module specialized for high energies, hex-dwba, that implements distorted and plane wave Born approximation.

Program summary #1

Program title: hex-db

Catalogue identifier: AETH_v1_0

Program summary URL: http://cpc.cs.qub.ac.uk/summaries/AETH_v1_0.html

Program obtainable from: CPC Program library, Queen's University, Belfast, N. Ireland

Licensing provisions: Standard CPC licence, <http://cpc.cs.qub.ac.uk/licence/licence.html>

No. of lines in distributed program, including test data etc.: 30367

No. of bytes in distributed program, including test data etc.: 232032

Distribution format: tar.gz

Programming language: C++11

Operating system: Any system with a C++11 compiler (e.g. GCC 4.8.1; tested on OpenSUSE 13.1 and Windows 8).

RAM: Test run 3 MiB.

CPC Library Classification: 2.4 Electron scattering

External libraries: GSL [49], FFTW3 [52], SQLite3 [46]. All of the libraries are open-source and maintained.

Nature of problem: Extraction of derived (observable) quantities from partial-wave T -matrices.

Method of solution: Simple algebraic operations and angular summations of the scattering T -matrices.

Additional comments: Command-line interface to a database shared between several computational backends.

Running time: Mostly less than a second.

[☆] This paper and its associated computer program are available via the Computer Physics Communication homepage on ScienceDirect (<http://www.sciencedirect.com/science/journal/00104655>).

^{*} Corresponding author. Tel.: +420 723716589.

E-mail addresses: jakub.benda@seznam.cz (J. Benda), karel.houfek@mff.cuni.cz (K. Houfek).

Program summary #2*Program title:* hex-dwba*Catalogue identifier:* AETH_v1_0*Program obtainable from:* CPC Program library, Queen's University, Belfast, N. Ireland*Programming language:* C++11*Operating system:* Any system with a C++11 compiler (e.g. GCC 4.8.1; tested on OpenSUSE 13.1 and Windows 8).*RAM:* Test run 7.5 MiB.*CPC Library Classification:* 2.4 Electron scattering*External libraries:* GSL [49], CLN [48], optionally HDF5 [53]. All of the libraries are open-source and maintained.*Nature of problem:* Perturbative solution of electron–hydrogen scattering for high energies.*Solution method:* Born approximation of the first order, with optional distortion of partial waves by the target potential.*Running time:* Test run consisting of 60 successive launches of the program took 9 min on Intel Core i7-3770K 3.5 GHz.

© 2014 Elsevier B.V. All rights reserved.

1. Introduction

The scattering event between a free electron and a neutral hydrogen atom in the ground or excited state is frequently encountered at least in two physics fields concerned with plasma: the tokamak physics [1,2] and the stellar astrophysics [3] or astrophysics of the interstellar medium in the early universe [4]. For this reason, there is still a need for reliable datasets for different reaction channels of the collision. The first mentioned case – dense plasma – is actually beyond a simple approximation of an isolated system, which is used in most works concerned with electronic scattering of atoms, because the densities in industrial plasmas can reach high values that would require the neighboring atoms to be also involved in the model. Such simulation then enforces even more simplifications than a low-density problem, e.g. the Debye-shielding averaging approach. In the stellar atmospheres, we can consider collisions to be isolated to much better approximation, because the densities are several orders lower (cf. [5,6]).

In stellar astronomy the microscopical data provided by the scattering theory are used together with optical measurements to obtain a detailed information about the particle processes occurring during significant solar events, most notably the solar flares. During a solar flare the released energy produces an amount of accelerated particles that hit denser shells of the solar atmosphere and may excite and de-excite the neutral hydrogen gas. Resulting radiation may depend on the direction of bombardment and observation; it can be partially polarized [7]. In this way particle collisions provide a means of observation not only on the sub-atomic, but also on the astrophysical scales.

Today, the electron–atom scattering is a well established research field and many, if not most, of its problems have already been given such a profound attention in the past that they are considered effectively solved. Particularly the case of electron–hydrogen–atom collisions received attention since the very dawn of the quantum physics. Starting with the pioneering works of Massey and Mohr [8–12] that used both close-coupling expansion and perturbative approach (Born approximation), this physics field evolved by development of several sophisticated methods as, among others, the straightforward close coupling [13–17], *R*-matrix [18,19], converged close coupling [20,21], time-dependent close coupling [22] and exterior complex scaling [23–25]. Also, the

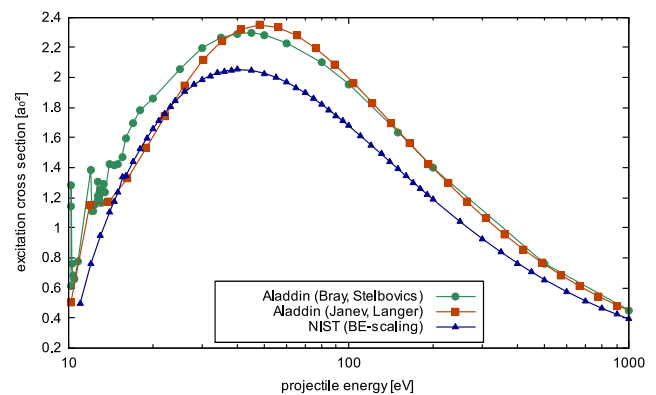


Fig. 1. Comparison of three datasets for integral cross section of the reaction $e^- + \text{H}(1s) \rightarrow e^- + \text{H}(2p)$, summed over possible resulting magnetic quantum numbers of the atom. The database Aladdin [28] contains two differing datasets for this transition taken from [29,30]. The NIST database [31] contains data from [32], which are also different. Variations reach more than 10%.

high energy limits have been investigated in the works on eikonal approximation [26], higher-order distorted wave Born approximation [27] and others. However, despite the wide range of available methods and computer programs, there is still no complete database or freely available and generally accessible computer package that could be used for comfortable generation of data by the applied researchers. An example of data from two on-line state-of-the-art databases is shown in Fig. 1. Apparently, their content is not fully compatible. Moreover, they contain only (some) integral cross sections and not other data, like differential cross sections.

Some of the existing programs are discussed in Section 3, illustrating the need of a new specialized code dealing with electron–hydrogen collisions. Our package is then introduced in Section 4. The database and its interface are discussed in Section 5, and the high-energy code in Section 6. Finally, Section 7 contains some examples of data produced by the high-energy codes.

2. Electron–hydrogen scattering

Being composed of three particles, the system (p^+, e^-, e^-) does not have a simple solution, neither classically nor quantumly; thus

all published methods are either fully numerical or rely on some kind of approximation to achieve at least semi-analytical outcome (the Born approximation would be one of the examples). First of all, the problem can be simplified by assumption that $m_p \gg m_e$, i.e. by neglecting the influence of electrons on the movement of the proton. This introduces an error of $\sim 5\%$, which is well below any distinguishing ability of the applied research fields. Still the principal difficulty remains and that is the correlation in the movement of the electrons. Whereas the movement of a particle in an external field can be solved more or less easily, two particles acting on each other in a comparable field of a third, heavy particle lead in the quantal context to a much more complicated equation due to the presence of the two-electron potential $V_{12} = |\mathbf{r}_1 - \mathbf{r}_2|^{-1}$

$$(\hat{H}_1 + \hat{H}_2 + V_{12}) \Psi_{\Gamma}(\mathbf{r}_1, \mathbf{r}_2) = E_{\Gamma} \Psi_{\Gamma}(\mathbf{r}_1, \mathbf{r}_2), \quad (1)$$

where

$$\hat{H}_i = -\frac{\nabla_i^2}{2} - \frac{1}{r_i} \quad (2)$$

is the one-particle Hamiltonian, i.e. the energy operator for the electron in the field of the proton. The atomic units are used, so that $\hbar = m_e = e = 4\pi\epsilon_0 = 1$, $c = 1/\alpha \sim 137$.

Eq. (1) can in principle contain the terms from the Breit–Pauli Hamiltonian that account for relativistic effects. In this work the relativistic effects have been neglected, though their implementation is one of further goals of the Hex project. Without the inclusion of spin-dependent terms some processes need to be disregarded, like the transitions in the fine structure. Quantitatively, the omission of the relativistic terms introduces an energy error proportional to $\sim (v/c)^2 \sim \alpha^2$, which is mostly even smaller than the error arising from the assumption of static proton.

Depending on the boundary condition used, Eq. (1) can yield different solutions. We are here primarily interested in scattering-type solutions of the asymptotic form

$$\Psi_{\Gamma}(\mathbf{r}_1, \mathbf{r}_2) = \Psi_{\Gamma_0}(\mathbf{r}_1, \mathbf{r}_2) + \sum_{\Lambda} f_{\Gamma\Lambda}(\hat{\mathbf{r}}_1) \frac{e^{ik_{\Gamma\Lambda}r_1}}{r_1} F_{\Lambda}(\mathbf{r}_2), \quad (3)$$

which is valid as $r_1 \rightarrow \infty$. The sum is over all open excitation channels Λ (here we considered the “second” electron to be bound). If the ionization channel is open one has to add term corresponding to the two-scattered-electron channel. From scattering amplitudes $f_{\Gamma\Lambda}$ we can determine observable quantities such as the excitation cross section.

Eq. (1) has also one bound state solution (it has the energy 0.75 eV below the energy of the isolated neutral hydrogen atom, see [33] and Fig. 2) and there are many resonances corresponding to metastable states of H^- with a finite lifetime. Energies of the doubly excited metastable H^- states (shown in Fig. 2) play a crucial role for explanation of sharp resonance structures in the low-energy electron–hydrogen scattering cross sections which are usually labeled by the electron configuration of these metastable states.

3. Available codes

The efforts to produce publicly available computer programs have a long tradition; however, many of the published codes remained academic deeds and did not spread well among applied researchers due to abundance of various input parameters and settings. Others have been published without a clear indication of their region of validity and, finally, some of the older programs are impossible to run today due to a drastic change of some Fortran dialects.

When starting work on the Hex project we inspected several available programs with the hope that there will be possibility of

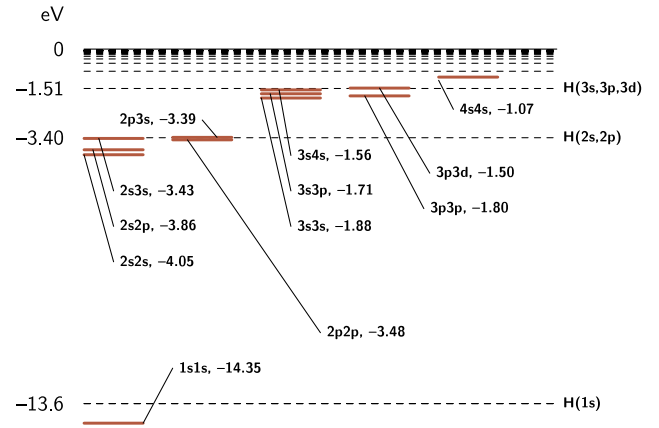


Fig. 2. Several energy levels of the ground and metastable doubly excited states of H^- . The energies of the ion have been taken from [34,35] and are given in electronvolts. For better orientation, the energy levels of the hydrogen atom are shown (dashed lines).

using them as the computational modules in the production of data. They were these programs:

- (low energies) RMATRIX1 [36], RmaX [37], BSR [38], 2DRMP [39], CefeusK [40],
- (high energies) Elsepa [41], Eikonal [42], Elastic [43], BetRT [44].

Unfortunately, the possibilities of most of them are strongly restricted. The high-energy codes work only for elastic scattering or for excitation to a few lowest lying states. The low-energy codes, mostly R -matrix packages, either require pseudostate expansion (that cannot be easily generated for the hydrogen case (BSR) or produces visible pseudoresonances (RmaX) or simply do not agree with output of the other codes (cf. Fig. 3). Eikonal even uses a commercial numerical library, which makes it difficult or nearly impossible to reproduce its results. High-energy programs are compared in Fig. 4.

For this reason we ended up implementing new specialized codes that are described in this series of articles.

4. Hex package outline

The Hex program package addresses several objections made above. First of all, it should contain well-documented and easy to use subprograms that would ultimately cover the whole energy range. Second, the coverage should be such that even at energies, where the energy-specific sub-methods overlap, the accuracy should never fall below 5%. Finally, the implementation uses only open-source libraries, so that the usage of the programs is never tied to a specific commercial black-box implementation.

Hex is composed of several parts. In the first place, it is the computational modules that serve to generate the data for a correct energy interval by solving the scattering problem in a valid approximation. At the moment it is the Born approximation for high energies, and direct solution of Eq. (1) in B-spline basis (with aid of exterior complex scaling) for low energies. The low-energy code is presented in the following article of this series. A simple scheme of the current state of the package is in Fig. 5.

Every computational module produces low-level scattering data that are stored in an intermediate storage. These data are the partial-wave T -matrices that together compose the full T -matrix of the scattering event,

$$T_{fi} = \sum_{\substack{\ell_1, \ell_2, \dots \\ A_1, \dots}} T_{fi, \ell_1, \ell_2, \dots}^{A_1, \dots} \mathcal{Y}_{\ell_1, \ell_2, \dots}^{A_1, \dots}, \quad (4)$$

where the indices ℓ_1 , etc., label all final state partial wave expansions that have been precomputed: e.g. expansion in angular

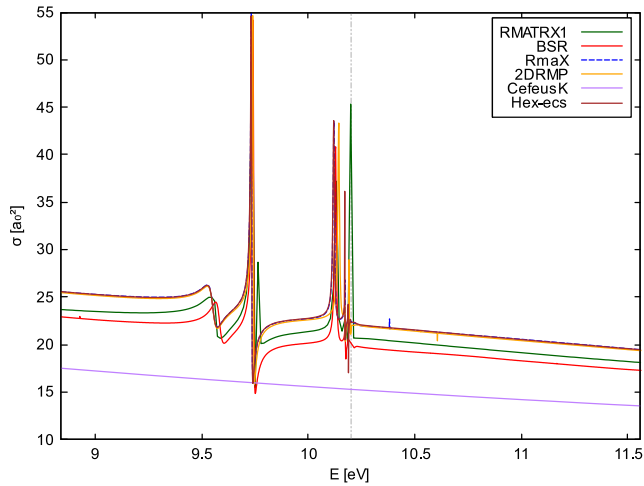


Fig. 3. Comparison of ground state elastic integral cross sections produced by several low-energy programs for a small energy interval containing an excitation threshold $n = 1 \rightarrow n = 2$ (light gray vertical line) and Feshbach resonances in its vicinity. Though the results of every code are as converged as possible, the curves still differ slightly, both in vertical and horizontal directions. Only RmaX and 2DRMP agree with each other, though these two exhibit some numerical fluctuations (pseudoresonances) around 10.5 eV. CefeusK is an experimental code which does not have ambitions to fully describe the electron–hydrogen scattering anyway. The last data row, called hex-ecs, that coincides with RmaX and 2DRMP (except for the pseudoresonances or numerical artifacts around 10.5 eV) is the cross section computed by the low-energy module of Hex. It is introduced in the second article of this series.

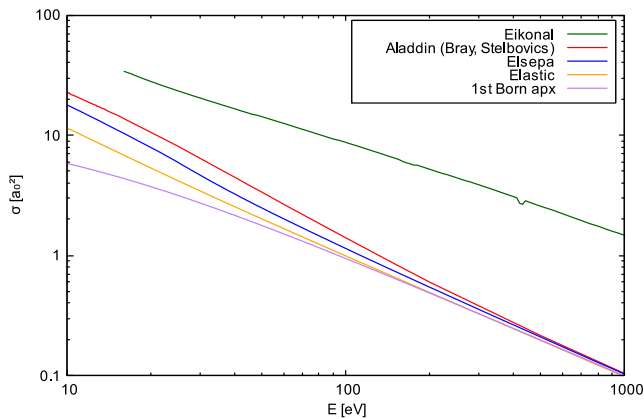


Fig. 4. The same process as in Fig. 3 but for energies from 10 eV above. The high-energy codes start to agree with each other (and with data from Aladdin [29]) from the energy ~ 1000 eV. This is coincidentally also an energy, for which the first Born approximation starts to give valid results. An exception are the results of Eikonal, which relies on two closed proprietary libraries, that may have undergone some changes since the publication of the program code. The bump on the Eikonal's curve is a persistent numerical artifact.

momentum of the single outgoing electron in elastic collision, or angular momenta of two outgoing electrons after an ionizing collision. The symbol \mathcal{Y} stands for the corresponding angular function, its upper indices for total (conserved) quantum numbers, like angular momentum or spin. Two examples may be

$$T_{fi}^S(\hat{\mathbf{k}}) = \sum_{\ell L} T_{fi,\ell}^{LS} Y_{\ell}^{m_i - m_f}(\hat{\mathbf{k}}) \quad (5)$$

for expansion of one-outgoing-particle T -matrix (used in hex-pwba2, hex-dwba and hex-ecs for elastic scattering and excitation) and

$$T_{fi}^S(\hat{\mathbf{k}}_1, \hat{\mathbf{k}}_2) = \sum_{\ell_1 \ell_2 L} T_{fi,\ell_1 \ell_2}^{Lm_i S} \mathcal{Y}_{\ell_1 \ell_2}^{Lm_i}(\hat{\mathbf{k}}_1, \hat{\mathbf{k}}_2) \quad (6)$$

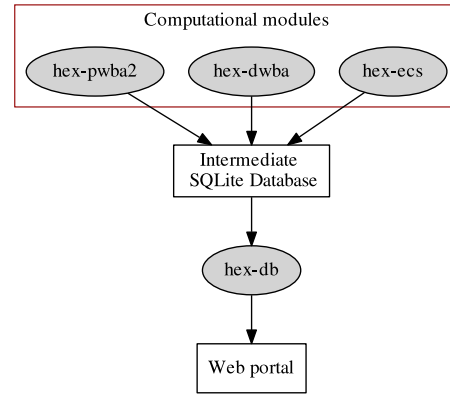


Fig. 5. Layout of the Hex package showing sample computational modules producing data for the intermediate storage and the command-line interface.

for expansion of T -matrix of a two-outgoing-particle channel (used in hex-ecs for ionization). The spherical harmonic function $Y_{\ell}^m(\vartheta, \varphi)$ depends on φ only through a phase factor which is identical to all partial waves. In Hex it is thus ignored altogether ($\varphi \equiv 0$).

The partial wave expansion (4) may need a large amount of contributions, particularly in the case of high energies. However, higher partial waves, starting from some total angular momentum L_0 , can be accurately modeled by the Born approximation (see e.g. [45]) thanks to the separation of the particles by the centrifugal barrier. Eq. (5) can be thus approximated by the form

$$\begin{aligned} T_{fi}^S(\vartheta) &= \sum_{L=0}^{L_0} \sum_{\ell} T_{fi,\ell}^{LS} Y_{\ell}^{m_i - m_f}(\vartheta) + \sum_{L=L_0+1}^{\infty} \sum_{\ell} T_{fi,\text{Born},\ell}^{LS} Y_{\ell}^{m_i - m_f}(\vartheta) \\ &= T_{fi,\text{Born}}^S(\vartheta) + \sum_{L=0}^{L_0} \sum_{\ell} (T_{fi,\ell}^{LS} - T_{fi,\text{Born},\ell}^{LS}) Y_{\ell}^{m_i - m_f}(\vartheta). \end{aligned} \quad (7)$$

This is the Born subtraction method for acceleration of the partial wave series. For correct description of inelastic transitions even at high angular momenta it is necessary to use the second-order Born approximation, which includes the coupling to continuum intermediate states. Born subtraction (7) is implemented in hex-db for discrete transitions by storing the partial waves $T_{fi,\text{Born},\ell}^{LS}$ next to the accurate T -matrices $T_{fi,\text{Born}}^{LS}$ and also by storing the angle-dependent function $T_{fi,\text{Born}}^S(\vartheta)$. These can be computed by custom codes or by the intermediate-energy module hex-pwba2 that will be published as a third article of this series.

For the storage format the SQLite database [46] has been chosen, so that the data can be retrieved and modified by a standardized set of simple SQL commands. The T -matrices are internally stored in a table indexed by collision quantum numbers ($n_i, l_i, m_i, n_f, l_f, m_f, E_i$, etc.) and existing management tools for these databases allow for easy

- addition, removal and updates of stored data items,
- structured query for more complicated combinations of the data items (e.g. the cross sections) and
- upgrade of data format, if necessary in the future.

5. Interface program

The interface program accepts all input data from the command line and from the standard input to allow a straightforward usage e.g. as a web-interface backend, like the one at <http://utf.mff.cuni.cz/data/hex>. It can be used to extract several derived scattering quantities listed further in this section. Moreover, it is developed in an object-oriented design that is easily extensible by other quantities.

Table 1

Required input quantum numbers for hex-db for computation of every implemented derived scattering quantity. Bullet symbols mark required numbers that are to be supplied by a command line switch, "--ni=1" or "--ni 1". Asterisks also mark required numbers, but these can be optionally read from standard input, so that more values can be specified: "echo 1.1 1.2 1.3 | hex-db... --Ei". Asterisk for impact energy also allows us to use "--Ei=-1" which will force the program to compute the selected quantity for every energy available in the database. The value E_{share} is the ratio between energies of the outgoing electrons.

Name	n_i, l_i, m_i	n_f, l_f, m_f	L	S	E_i	E_{share}	$\ell/\ell_1, \ell_2$	ϑ/dirs
<i>T</i> -matrix	•	•	•	•	*		•	
Scattering amplitude	•	•	•	•	•			*
Differential cross section	•	•	•	•	•			*
Integral cross section	•	•	•	•	*			
Complete cross section	•	•			*			
Extrapolated cross section	•	•			*			
Total cross section	•				*			
Momentum transfer	•	•	•	•	*			
Collision strength	•	•	•	•	*			
(e, γ) correlation parameters	just n_i	just n_f			*			
Ionization amplitude	•			•	•			*
Ionization f	•		•	•	•	*	•	
Triple differential cross section	•			•	•			*

A typical usage of the interface program is demonstrated in the test run and consists of the following steps: first, a new, empty database is created, that contains all necessary internal tables:

```
> hex-db [--database <name>] --new
```

The switch specifying the database name is optional; *hex.db* is the default name if omitted. Next, one imports data computed by one of the modules:

```
> hex-db [--database <name>] --import <SQL file>
```

The data have the form of SQL batch files, i.e. they are human readable and editable text files containing SQL commands for insertion of new data items. Typical example would be a set of lines similar to this annotated one:

```
INSERT OR REPLACE INTO "tmat" VALUES
(
  1,0,0,          ...  ni, li, mi
  3,1,-1,        ...  nf, lf, mf
  3, 1, 4.0, 4,  ...  L, S, Ei, ℓ
  1.52,3.25,     ...  Re Tfi,ℓLS, Im Tfi,ℓLS
  0.0,0.0       ...  Re Tfi,Born,ℓLS, Im Tfi,Born,ℓLS
);
```

This statement would insert $T_{\ell=4}^{LS} = 1.52 + 3.25i$ as the partial *T*-matrix for excitation from the ground state to 3p ($m_f = -1$) for impact energy $E = 4$ Ry, total angular momentum $L = 2$ and total spin $S = 1$. The total angular momentum L is used for low-energy data, where the scattering state is expanded also in total conserved quantum numbers.

The angle-dependent Born *T*-matrix $T_{f_i, \text{Born}}(\vartheta)$ is stored in a separate table "bornf" as a sequence of complex Chebyshev coefficients of its expansion in $x \equiv \cos \vartheta$, written as an SQLite *blob*, which is an advantageous form of storing binary data; every byte of the original sequence is written in hexadecimal representation. An example of a statement for insertion of some data to the table "bornf" is

```
INSERT OR REPLACE INTO "bornf" VALUES
(
  1,0,0,          ...  ni, li, mi
  3,1,-1,        ...  nf, lf, mf
  4.0,          ...  Ei
  x'0ab4f6ffc6...' ... first 5 bytes of data
);
```

Whenever the exact queried energy is missing in the database, a linear interpolation is done from the available data. If the requested

quantity is a cross section and the impact energy is above ionization threshold, i.e. not in a vicinity of a resonance, a cubic spline interpolation is done.

Computation or interpolation of e.g. the total cross section all the way from the *T*-matrices would be time expensive, so several key quantities are being automatically precomputed and stored in the database on every requested update:

```
> hex-db [--database <name>] --update
```

These *cache tables* are then used when querying for more complex data. It is also possible to use all three mentioned switches in one call, if necessary (illustrated in the test run). Other information can be found in the documentation and in the program help:

```
> hex-db --help # display full usage info
```

The interface program can also be used as a library for accessing the database from a separate code. If the source file *ui.cpp* is omitted, the rest can be compiled into a *shared-object* file (or directly linked to a derived program), with *hex-db.h* and *interfaces.h* containing the declarations of interface subroutines.

The main functionality of the interface is to query for derived scattering variables. The complete list of those that are implemented can be retrieved by

```
> hex-db --vars # list available quantities
```

In the rest of this section we define all currently implemented quantities. Table 1 shows which input quantum numbers are required for computation of the respective derived quantity. The test run shows typical usage of the program.

5.1. *T*-matrix, --tmat

The *T*-matrix of a discrete transition is simply the partial *T*-matrix $T_{f_i, \ell}^S$ as in Eq. (4). Values of the partial *T*-matrices are stored in the basic SQL table "tmat". The optional Born *T*-matrices are stored here as well.

5.2. Scattering amplitude, --scatamp

The scattering amplitude of a discrete transition is computed as a linear combination of correct *T*-matrices,

$$f_{f_i}^S = -\frac{1}{2\pi} \sum_{\ell L} T_{f_i, \ell}^{LS} Y_{\ell}^{m_i - m_f}. \quad (8)$$

If present, Born *T*-matrices are used to accelerate the series using the Born subtraction method (7).

5.3. Differential cross section, --dcs

The differential cross section is defined by scattering amplitude as

$$\frac{d\sigma_{fi}^S}{d\Omega} = \frac{k_f}{k_i} \frac{2S+1}{4} |f_{fi}^S|^2. \quad (9)$$

5.4. Integral cross section, --ics

Thanks to orthogonality of Legendre polynomials, the integral cross section of a discrete transition can be computed as the following sum of the correct T -matrices,

$$\sigma_{fi}^{LS} = \frac{k_f}{k_i} \frac{2S+1}{4} \frac{1}{4\pi^2} \sum_{\ell\ell'} T_{fi,\ell}^{LS} T_{fi,\ell'}^{L'S*}. \quad (10)$$

The same formula is used to compute the Born integral cross section $\sigma_{fi,\text{Born}}^{LS}$ from Born partial T -matrices $T_{fi,\text{Born},\ell}^{LS}$. For ionizing collisions we have,

$$\sigma_{fi}^{LS} = \sum_{\ell_1\ell_2} \int_0^{E/2} \frac{k_1 k_2}{k_i} |f_{\ell_1\ell_2}^{Lm_i S}|^2 dE_2. \quad (11)$$

The symbol $f_{\ell_1\ell_2}^{Lm_i S}$ is defined in Section 5.12. The integral cross section is one of the “cached” quantities—on every update it is being precomputed and stored in a dedicated SQL table `ics`, so that it can be used when querying for the value of σ_{fi}^{LS} .

5.5. Complete cross section, --ccs

The complete cross section (sometimes also called the *total* cross section) is defined as a simple sum of the integral cross sections over all total quantum numbers. When the Born subtraction method is used, we have

$$\sigma_{fi} = \sigma_{fi,\text{Born}} + \sum_{LS} (\sigma_{fi}^{LS} - \sigma_{fi,\text{Born}}^{LS}). \quad (12)$$

The complete Born cross section $\sigma_{fi,\text{Born}}$ is computed as

$$\sigma_{fi,\text{Born}} = \frac{k_f}{k_i} \frac{1}{4\pi^2} \int |T_{fi,\text{Born}}(\vartheta)|^2 d\Omega \quad (13)$$

by adaptive Clenshaw–Curtis quadrature.

5.6. Extrapolated cross section, --xcs

This option extrapolates the sum over L in (12) by the Aitken delta-squared process.

5.7. Total cross section, --tcs

The total cross section (sometimes also called the *grand total* cross section) is a sum of the complete cross sections with common initial state,

$$\sigma_i^{\text{tot}} = \sum_f \sigma_{fi}. \quad (14)$$

5.8. Momentum transfer, --momtf

The momentum transfer is defined by an angular integral of the differential cross section with an anisotropical weight function,

$$\eta_{fi}^{LS} = \int \frac{d\sigma_{fi}^{LS}}{d\Omega} (1 - \cos \vartheta) d\Omega. \quad (15)$$

5.9. Collision strength, --colls

Collision strength is the integral cross section defined in (10) or (11) scaled by angular multiplicities and by the projectile energy. It is thus symmetric in the indices $i \leftrightarrow f$ (reciprocity theorem).

$$\Omega_{fi}^{LS} = k_i^2 (2L+1)(2S+1) \sigma_{fi}^{LS}. \quad (16)$$

5.10. Electron–photon correlation parameters, --stokes

In electron–photon coincidence experiments several special variables are used. For a dipole-allowed transition ($|l_i - l_f| = 1$, e.g. $\text{H}(1s) \rightarrow \text{H}(2p)$) they are defined using following three basic statistical quantities:

$$\lambda = \langle |f_0^2| \rangle \left(\frac{d\sigma}{d\Omega} \right)^{-1}, \quad (17)$$

$$R = \text{Re} \langle f_1 f_0^* \rangle \left(\frac{d\sigma}{d\Omega} \right)^{-1}, \quad (18)$$

$$I = \text{Im} \langle f_1 f_0^* \rangle \left(\frac{d\sigma}{d\Omega} \right)^{-1}. \quad (19)$$

Here, we dropped the indices to keep the formulas compact. Nevertheless, the quantities f (scattering amplitudes) and $d\sigma/d\Omega$ (differential cross section) do depend on initial and final states. The angle brackets symbolize averaging over spin states (i.e. 75% of triplet result, 25% of singlet result) and the indices (zero or one) indicate whether the transition changed atomic magnetic quantum number (one) or did not (zero). *Reduced Stokes parameters* are then the components of the vector

$$\mathbf{P} = (2\lambda - 1; 2\sqrt{2}R; -2\sqrt{2}I), \quad (20)$$

linear polarization is the size of the projection of \mathbf{P} orthogonal to the third axis,

$$P_l = \sqrt{P_1^2 + P_2^2}, \quad (21)$$

charge cloud alignment is the angle parameter

$$\gamma = \frac{1}{2} \arg(P_1 + iP_2) \quad (22)$$

and *excitation coherence* is the magnitude of the vector \mathbf{P} ,

$$P^+ = |\mathbf{P}|. \quad (23)$$

All these numbers will be written out if the switch `--stokes` is used.

5.11. Ionization amplitude, --ionamp

The formulas for ionization amplitudes are given here for completeness, but their context is given in the second article, which describes the low-energy code. The ionization amplitude is

$$F^S(\mathbf{k}_1, \mathbf{k}_2) = \sum_{\ell_1\ell_2LM} i^{-\ell_1-\ell_2} e^{i(\sigma_1+\sigma_2)} f_{\ell_1\ell_2}^{Lm_i} \mathcal{Y}_{\ell_1\ell_2}^{Lm_i}, \quad (24)$$

where the symbol $f \equiv f(k_1, k_2)$ is the “radial part” of the ionization amplitude, because it depends only on magnitudes of the linear momenta, and its definition is given below. The bi-polar spherical functions $\mathcal{Y} \equiv \mathcal{Y}(\hat{\mathbf{k}}_1, \hat{\mathbf{k}}_2)$ are defined as

$$\mathcal{Y}_{\ell_1\ell_2}^{LM}(\hat{\mathbf{k}}_1, \hat{\mathbf{k}}_2) = \sum_m C_{\ell_1 m \ell_2 M-m}^{LM} Y_{\ell_1 m}(\hat{\mathbf{k}}_1) Y_{\ell_2, M-m}(\hat{\mathbf{k}}_2). \quad (25)$$

5.12. Radial part of ion. amp., --ionf

The radial part of ionization amplitude is, apart from some constant factors, essentially the T -matrix introduced in (6); cf. with

(24). This quantity is defined as a two-dimensional function of two linear momenta by a contour integral along a quarter-circle in the (r_1, r_2) -plane

$$f_{\ell_1 \ell_2}^{Lm_i S}(k_1, k_2) = \frac{2}{\sqrt{\pi}} \frac{\rho}{k_1 k_2} \int_0^{\pi/2} \mathcal{W}(r_1(\alpha), r_2(\alpha)) d\alpha \quad (26)$$

of the Wronskian of the solution and the product of Coulomb waves

$$\mathcal{W}(r_1, r_2) = \phi_1 \phi_2 \frac{\partial}{\partial \rho} \psi_{\ell_1 \ell_2}^{Lm_i S} - \psi_{\ell_1 \ell_2}^{Lm_i S} \frac{\partial}{\partial \rho} \phi_1 \phi_2. \quad (27)$$

Nevertheless, the momenta k_1 and k_2 for a physical system have to fulfill the energy conservation $k_1^2 + k_2^2 = 2(E_i - \Delta E_{\beta}^{\text{st}})$, so that f can be viewed as a one-dimensional function. As such it is also kept in the database—in a form of a set of Chebyshev expansion coefficients, encoded to an SQL *blob* (text string).

5.13. Triple differential c.s., --tdcs

The triple differential cross section (sometimes also called the fully differential cross section) is a generalization of the differential cross section from Section 5.3. It represents the density of probability of all final configurations of an ionized system. The definition is

$$d\sigma = \sum_S \frac{2S+1}{4} \frac{k_1 k_2}{k_i} |F^S|^2 d\hat{\mathbf{k}}_1 d\hat{\mathbf{k}}_2 dE_2. \quad (28)$$

The angles are specified by the switch “--dirs” as for example (other input has been omitted):

```
> hex-db --tdcs --dirs="(ϑ1, ϕ1, x1) (ϑ2, ϕ2, x2)"
or
```

```
> echo "(ϑ1, ϕ1, x1) (ϑ2, ϕ2, x2)" | hex-db --tdcs
```

The angles ϑ_i and ϕ_i are the polar and azimuthal ejection angles of the i th ejected electron with respect to the incoming electron direction and the energy fraction x_i is used to compute its energy as a part of the total available energy,

$$E_i = (E_1 + E_2) \frac{x_i}{x_1 + x_2}. \quad (29)$$

6. High-energy code

Hex-dwba is a simple code based on the first-order Born approximation, which computes the T -matrix as the first term of the Born series. It can be run both in the plane wave mode and in the distorted wave mode.

6.1. Plane wave mode

In the plane wave Born approximation the T -matrix is given by

$$T = \left\langle \beta_f(\mathbf{r}_2) \psi_f(\mathbf{r}_1) \left| \left(\frac{1}{r_{12}} - \frac{1}{r_2} \right) \right| \psi_i(\mathbf{r}_1) \beta_i(\mathbf{r}_2) \right\rangle, \quad (30)$$

where ψ stands for the hydrogen bound state and β is the projectile plane wave. Eq. (30) could in principle contain the exchange term; however, in the domain of validity of the Born approximation the exchange is utterly negligible. The partial wave expansion in accord with Eq. (5) then reads

$$T_{\beta_i}^{(S)} = \sum_{L\ell_f} T_{\ell_f}^{L(S)} Y_{\ell_f}^{m_i - m_f} = \sum_{L\ell_f \ell_i} i^{\ell_i - \ell_f} \frac{(4\pi)^2}{k_i k_f} \sqrt{\frac{2\ell_i + 1}{4\pi}} \times C_{\ell_f m_f \ell_i m_i - m_f}^{Lm_i} C_{\ell_i m_i \ell_i \ell_i}^{Lm_i} f_{\ell_f \ell_i \ell_i; L}^{\lambda} A_{\beta_i}^{\lambda} Y_{\ell_f}^{m_i - m_f}, \quad (31)$$

where

$$A_{\beta_i}^{\lambda} = \int \hat{j}_{\ell_i}(k_i r_2) \hat{j}_{\ell_f}(k_f r_2) V_{\beta_i}^{\lambda}(r_2) dr_2, \quad (32)$$

$$V_{\beta_i}^{\lambda}(r_2) = \int \psi_f(r_1) \psi_i(r_1) \left(\frac{r_{<}^{\lambda}}{r_{>}^{\lambda+1}} - \frac{\delta_{\lambda}^0}{r_2} \right) dr_1, \quad (33)$$

$C_{\ell_1 m_1 \ell_2 m_2}^{LM}$ is the Clebsch–Gordan coefficient and

$$f_{\ell_1 \ell_2 \ell'_1 \ell'_2; L}^{\lambda} = (-1)^{L+\ell_2+\ell'_2} [\ell_1 \ell_2 \ell'_1 \ell'_2] \begin{Bmatrix} \ell_1 & \ell_2 & L \\ \ell'_2 & \ell'_1 & \lambda \end{Bmatrix} \times \begin{pmatrix} \ell_1 & \lambda & \ell'_1 \\ 0 & 0 & 0 \end{pmatrix} \begin{pmatrix} \ell_2 & \lambda & \ell'_2 \\ 0 & 0 & 0 \end{pmatrix}, \quad (34)$$

where $[\ell_1 \ell_2 \ell'_1 \ell'_2] \equiv \sqrt{(2\ell_1 + 1)(2\ell_2 + 1)(2\ell'_1 + 1)(2\ell'_2 + 1)}$, parentheses denote the Wigner 3j-symbol [47, Section 3.7] and the braces the 6j-symbol [47, Section 6.1]. The inner integral $V_{\beta_i}^{\lambda}$ is being computed exactly using rational arithmetic provided by the library CLN [48]; the outer integral $A_{\beta_i}^{\lambda}$ containing Riccati–Bessel functions $\hat{j}_{\ell}(kr)$ is being computed by the adaptive Gauss–Kronrod routine from GSL [49].

The plane wave mode is activated by the command line option “--nodistort”; otherwise the distorted wave mode is assumed.

6.2. Distorted wave mode

In order to describe the collision better and still keep just the first term of the perturbation expansion, the potential can be split into two parts: one that will be treated perturbatively as before and one that will be directly included in the solution of the scattering states. The states χ will then differ from exact plane waves β —they will acquire some *distortion*. Hence we have “distorted wave” Born approximation. The equation for a distorted wave is

$$\left(-\frac{\nabla^2}{2} + U_{\alpha} \right) \chi_{\alpha} = E_{\alpha} \chi_{\alpha}, \quad (35)$$

where the distorting potential U_{α} is chosen as the spherical average of the potential V_{12} felt by the projectile in the initial ($\alpha = i$) or final ($\alpha = f$) state,

$$U_{\alpha}(r_2) = \frac{1}{4\pi} \int \int \psi_{\alpha}(\mathbf{r}_1) \left(\frac{1}{r_{12}} - \frac{1}{r_2} \right) \psi_{\alpha}(\mathbf{r}_1) d^3 \mathbf{r}_1 d\Omega_2. \quad (36)$$

The solutions of (35) are chosen such that their asymptotic form for $r \rightarrow \infty$ is that of scattering states,

$$\chi_{\ell}(k, r) \longrightarrow e^{i\delta_{\ell}(k)} \sin \left(kr - \frac{\pi\ell}{2} + \delta_{\ell}(k) \right). \quad (37)$$

The first-order scattering T -matrix is

$$T^S = T_{\text{dir}} + (-1)^S T_{\text{exc}}, \quad (38)$$

where

$$T_{\text{dir}} = \langle \chi_f \psi_f | V | \psi_i \chi_i \rangle + \langle \chi_f | U_f | \beta_i - \chi_i \rangle \delta_{\beta_i}, \quad (39)$$

$$T_{\text{exc}} = \langle \psi_f \chi_f | V | \psi_i \chi_i \rangle - \langle \chi_f | U_f | \psi_i \rangle \langle \psi_f | \chi_i \rangle. \quad (40)$$

In the program the distorted waves χ are being pre-computed by an adapted Cash–Karp Runge–Kutta routine from GSL on a grid terminated at sufficiently large radius r_{max} , where the distorting potential is negligible. Optionally, the r_{max} can be specified on the command line. Then, during numerical Gauss–Chebyshev quadrature they are either interpolated from the stored values using the cubic spline interpolation routine from GSL or approximated by the asymptotic form (37) for $r > r_{\text{max}}$.

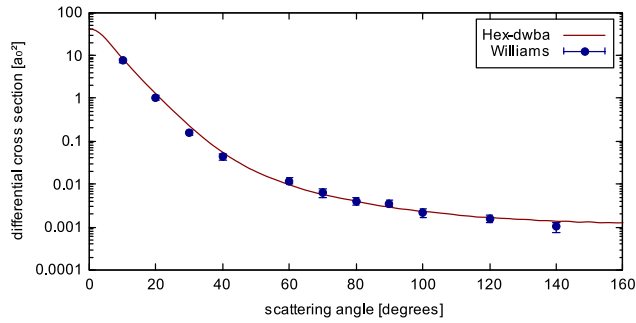


Fig. 6. The differential cross section for impact excitation $H(1s) \rightarrow H(2p)$ at impact energy $E_i = 4$ Ry as computed by hex-dwba. The results were averaged over spins and summed over final magnetic quantum numbers. The experimental data come from the measurement of Williams [50].

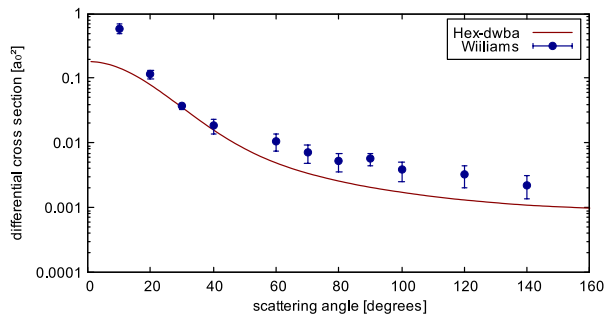


Fig. 7. The differential cross section for impact excitation $H(1s) \rightarrow H(2s)$ at impact energy $E_i = 4$ Ry as computed by hex-dwba. The results were averaged over spins and summed over final magnetic quantum numbers. The experimental data come from the measurement of Williams [50]. This particular measurement may be flawed, though, because the experimental data – when integrated – result in considerably higher integral cross section compared to the value from Aladdin [28].

7. Results

The high-energy codes implement well-known methods, so this section is here to show the range of validity of these methods. It is known that the first order of the Born series contains sufficient information at energies much larger than the ionization threshold. In the intermediate region that spans, approximately, the interval from 50 eV to 1 keV, the higher-order corrections are rising on importance.

Also, the accuracy of the approximation is limited by the scattering transition that is being investigated. The cross section for dipole-allowed transitions (e.g. $H(1s) \rightarrow H(2p)$) receives most of the contribution from the first-order processes even at lower energies, whereas the others (e.g. $H(1s) \rightarrow H(2s)$) require inclusion of higher-order corrections at a considerable wider range of energies.

Experimental data for comparison are scarce in the high-energy limit. We have chosen the impact energy 54.4 eV for demonstration of the first-order results; see Figs. 6 and 7. The computation leading to the first one is also presented in Appendix A as a test run. Fig. 8 presents a comparison of energy dependence of integral cross sections.

8. Conclusion

In this article we have presented the structure of the computer package Hex that is being developed with the intention of simulating all processes in the electron–hydrogen scattering, for all energies, so that a complete database can be produced for use in applied research (stellar physics, plasma physics, etc.). Hex consists of computational modules (solvers) that can be used for different

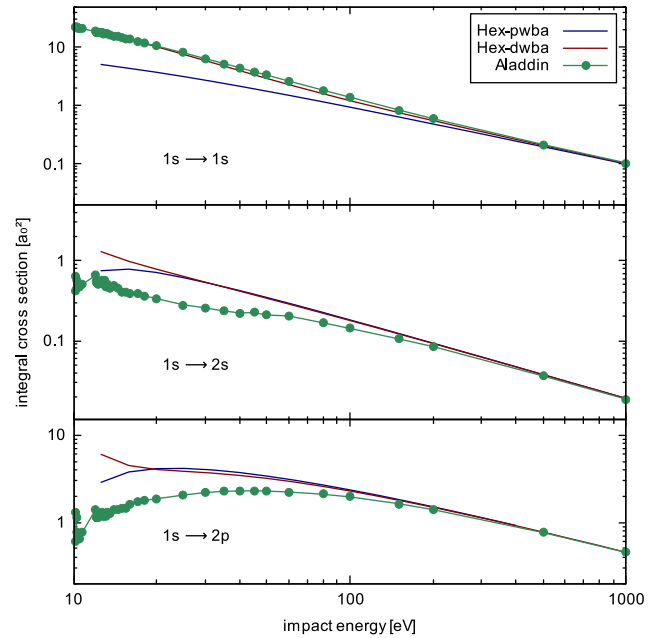


Fig. 8. The integral cross section dependence on impact energy for several transitions. The data obtained by the Hex module hex-dwba with or without distortion (denoted by “hex-pwba” in the second case) are compared with converged close coupling computation (CCC) from the database Aladdin [28]. At 54.4 eV the Born approximation differs from CCC also in the case of $1s \rightarrow 2p$ transition, which seems to contradict well behaved Fig. 6. However, DWBA overestimates the cross sections for $\vartheta \rightarrow 0$, which is not apparent in Fig. 6 due to the absence of measurement. Anyway, from the energy ~ 1 keV the theories provide the same results.

energy domains and of the program hex-db, which is a command-line interface with rich usage in scripting. The link between the solvers and the interface is a shared database of the SQLite format, that can be explored and processed also by many standard tools.

The low-energy code, that uses exterior complex scaling, is presented in the second article of this series. The intermediate-energy code, that uses second order Born approximation and can be used to enhance the low energy T -matrices by the method of Born subtraction, will be presented in the third article.

As the next step we plan to generate datasets, so that data from our programs are accessible even without the burden of running the software. Our intent is also to provide the data within the VAMDC infrastructure [51].

Acknowledgments

The work was supported by the Charles University in Prague, project GA UK No 730214, and by Grant SVV-260089.

The access to computing and storage facilities owned by parties and projects contributing to the National Grid Infrastructure MetaCentrum, provided under the programme “Projects of Large Infrastructure for Research, Development, and Innovations” (LM2010005) is greatly appreciated.

The access to the CERIT-SC computing and storage facilities provided under the programme Center CERIT Scientific Cloud, part of the Operational Program Research and Development for Innovations, reg. no. CZ. 1.05/3.2.00/08.0144 is greatly appreciated.

Appendix. Test run

The test run computes T -matrices for the electron impact excitation of hydrogen from the ground state to the state 2p (for all final magnetic quantum numbers). The program is launched by

```
> hex-dwba 1 0 2 1 4.0 0 1000
```

```

BEGIN TRANSACTION;
INSERT OR REPLACE INTO "tmat" VALUES (1,0,0, 2,1,-1, 0,0, 4.0, 1, 7.870811e-01,2.214352e-01, 0,0);
INSERT OR REPLACE INTO "tmat" VALUES (1,0,0, 2,1,-1, 0,1, 4.0, 1, 5.217714e-01,1.467937e-01, 0,0);
INSERT OR REPLACE INTO "tmat" VALUES (1,0,0, 2,1,0, 0,0, 4.0, 1, -7.870811e-01,-2.214352e-01, 0,0);
INSERT OR REPLACE INTO "tmat" VALUES (1,0,0, 2,1,0, 0,1, 4.0, 1, -5.217714e-01,-1.467937e-01, 0,0);
INSERT OR REPLACE INTO "tmat" VALUES (1,0,0, 2,1,1, 0,0, 4.0, 1, 7.870811e-01,2.214352e-01, 0,0);
INSERT OR REPLACE INTO "tmat" VALUES (1,0,0, 2,1,1, 0,1, 4.0, 1, 5.217714e-01,1.467937e-01, 0,0);
COMMIT;

```

Fig. A.9. Several first rows of the hex-dwba test run output file *dwba-1-0-2-1-L0-E4.sql*.

where the numbers passed to hex-dwba stand for: n_i , l_i , n_f , l_f , E_i , L and r_{\max} . The last (optional) parameter r_{\max} is the maximal radial distance to which to compute the wave functions $\chi_\ell(k, r)$; this can be used to override the implicit value determined from the distorting potential. Note that the running time is rather high (several minutes), due to the fact that we are dealing with the P-state, so that many partial waves are necessary. Excitation to an S-state would be computed much faster (less partial waves would be necessary); however, the agreement with the experiment would be worse, because a large contribution to the cross section comes from a second-order effect—from the intermediate transition $H(1s) \rightarrow H(np) \rightarrow H(2s)$. The program output is the SQL batch file displayed in Fig. A.9. It can be inserted into the database manually using the sqlite3 program

```
> sqlite3 hex.db < dwba-1-0-2-1-E4-L0.sql
```

or, preferably, by hex-db itself. The following bash script runs the solver for several partial waves and also illustrates the creation of the database and the extraction of the differential cross section:

```

#!/bin/bash

# remove old data
rm -f hex.db *.log *.sql *.dcs

# compute partial waves up to L = 70
for L in $(seq 0 70); do
  hex-dwba 1 0 2 1 4. $L 1000 \
    | tee -a test-run.log
done

# create a new database
hex-db --new

# fill the database with the data
for SQL in *.sql; do
  hex-db --import $SQL
done

# retrieve DCS for each S and final atomic M
for Mf in -1 0 1; do
  for S in 0 1; do
    seq 0 180 | hex-db --dcs \
      --ni=1 --li=0 --mi=0 \
      --nf=2 --lf=1 --mf=$Mf \
      --S=$S --Ei=4. \
      | grep -v '# ' \
      > dwba-1s-2p$Mf-S$$S.dcs
  done
done

# sum all cross sections (= even columns)
paste *.dcs | awk '{
  sum=0;
  for (i=1; i<=NF; i++)

```

```

  if (i % 2 == 0)
    sum += $i;
  print $1,sum;
}' > dwba-1s-2p.dcs

```

Note that the angles are given in degrees unless --Aunits=rad is given on the command line. Similarly, energy is given in Rydberg units unless --Eunits is set to "a.u." or "eV". Finally, the cross sections are printed in atomic units (Bohr radii squared, a_0^2) unless --Tunits is set to "cgs", then they are in cm^2 .

The resulting file *dwba-1s-2p.dcs* will contain two columns: angles in degrees and the summed differential cross section. Data compared with experiment are in Fig. 6.

References

- [1] T.T. Scholtz, et al., *Mon. Not. R. Astron. Soc.* 242 (1990) 692–697.
- [2] H. Anderson, et al., *J. Phys. B: At. Mol. Opt. Phys.* 33 (2000) 1255.
- [3] M. Karlický, J. Kašparová, P. Heinzl, *Astron. Astrophys.* 416 (2004) L13–L16.
- [4] S.R. Furlanetto, S.P. Oh, F.H. Briggs, *Phys. Rep.* 433 (2006) 181–301.
- [5] M.J. Aschwanden, et al., *Solid Phys.* 210 (2002) 383–405.
- [6] M. Murakami, J. Callen, L. Berry, *Nucl. Fusion* 16 (1976) 347.
- [7] A. Werner, K.-H. Scharfner, *J. Phys. B: At. Mol. Opt. Phys.* 29 (1996) 125.
- [8] H.S.W. Massey, C.B.O. Mohr, *Proc. R. Soc. Lond. A* 132 (1931) 605–630.
- [9] H.S.W. Massey, C.B.O. Mohr, *Proc. R. Soc. Lond. A* 136 (1932) 289–311.
- [10] H.S.W. Massey, C.B.O. Mohr, *Proc. R. Soc. Lond. A* 139 (1933) 187–201.
- [11] H.S.W. Massey, C.B.O. Mohr, *Proc. R. Soc. Lond. A* 140 (1933) 613–636.
- [12] H.S.W. Massey, C.B.O. Mohr, *Proc. R. Soc. Lond. A* 146 (1934) 880–900.
- [13] P.G. Burke, H.M. Schey, *Phys. Rev.* 126 (1962) 147–162.
- [14] P.G. Burke, D.F. Gallaher, S. Geltman, *J. Phys. B: At. Mol. Phys.* 2 (1969) 1142.
- [15] S. Geltman, P.G. Burke, *J. Phys. B: At. Mol. Phys.* 3 (1970) 1062.
- [16] P.G. Burke, T.G. Webb, *J. Phys. B: At. Mol. Phys.* 3 (1970) L131.
- [17] P.G. Burke, J.F.B. Mitchell, *J. Phys. B: At. Mol. Phys.* 6 (1973) 320.
- [18] P.G. Burke, 2011.
- [19] O. Zatsarinny, K. Bartschat, *J. Phys. B: At. Mol. Opt. Phys.* 46 (2013) 112001.
- [20] I. Bray, A.T. Stelbovics, *Phys. Rev. A* 46 (1992) 6995.
- [21] D.V. Fursa, I. Bray, *Phys. Rev. Lett.* 100 (2008) 113201.
- [22] J. Colgan, et al., *Phys. Rev. A* 65 (2002) 042721.
- [23] T.N. Rescigno, et al., *Science* 286 (1999) 2474–2479.
- [24] C.W. McCurdy, F. Martín, *J. Phys. B: At. Mol. Opt. Phys.* 37 (2004) 917.
- [25] P.L. Bartlett, *J. Phys. B: At. Mol. Opt. Phys.* 39 (2006) R379.
- [26] E.J. Mansky, M.R. Flannery, *J. Phys. B: At. Mol. Opt. Phys.* 23 (1990) 4549.
- [27] A.E. Kingston, H.R.J. Walters, *J. Phys. B: At. Mol. Phys.* 13 (1980) 4633.
- [28] R.A. Hulse, The ALADDIN atomic physics database system, *AIP Conf. Proc.* 206 (1990) 63–72.
- [29] I. Bray, A.T. Stelbovics, *Adv. At. Mol. Opt. Phys.* 35 (1995) 209–254.
- [30] R.K. Janev, W.D. Langer, K. Evans, D.E. Post, *Elementary processes in hydrogen-helium plasmas*, in: *Springer Series on Atoms and Plasmas*, Springer-Verlag, Berlin, Heidelberg, New York, 1987.
- [31] Y.-K. Kim, et al. *Electron-Impact Cross Sections for Ionization and Excitation*, NIST Standard Reference Database 107 (last update: 2005).
- [32] Y.-K. Kim, *Phys. Rev. A* 64 (2001) 032713.
- [33] A. Rau, *J. Astrophys. Astron.* 17 (1996) 113–145.
- [34] M. Biaye, M. Dieng, I. Sakho, A. Konte, A.S. Ndao, A. Wague, *Chin. J. Phys.* 47 (2008) 166–172.
- [35] A. Bùrgers, E. Lindroth, *Eur. Phys. J. D: At. Mol. Opt. Plas. Phys.* 10 (2000) 327–340.
- [36] K.A. Berrington, W.B. Eissner, P.H. Norrington, *Comput. Phys. Commun.* 92 (1995) 290–420.
- [37] K.A. Berrington, *The RmaX Network: R-matrix calculations for X-ray atomic processes*, in: M.A. Bautista, T.R. Kallman, A.K. Pradhan (Eds.), *Atomic Data Needs for X-ray Astronomy*, 2000, pp. 65–67.
- [38] O. Zatsarinny, *Comput. Phys. Commun.* 174 (2006) 273–356.
- [39] N. Scott, et al., *Comput. Phys. Commun.* 180 (2009) 2424–2449.
- [40] J. Horáček, J. Bok, *Comput. Phys. Commun.* 59 (1990) 319–323.
- [41] F. Salvat, A. Jablonski, C.J. Powell, *Comput. Phys. Commun.* 165 (2005) 157–190.

- [42] E. Mansky, M. Flannery, *Comput. Phys. Commun.* 88 (1995) 249–277.
- [43] D. Schultz, C. Reinhold, *Comput. Phys. Commun.* 114 (1998) 342–355.
- [44] A. Burgess, C.T. Whelan, *Comput. Phys. Commun.* 47 (1987) 295–304.
- [45] I.E. McCarthy, A.T. Stelbovics, *Phys. Rev. A* 28 (1983) 2693.
- [46] M. Owens, *The Definitive Guide to SQLite (Definitive Guide)*, Apress, Berkeley, CA, 2006.
- [47] A.R. Edmonds, *Angular Momentum in Quantum Mechanics*, Princeton University Press, Princeton, New Jersey, 1957.
- [48] B. Haible, R.B. Kreckel, *Class library for numbers*. <http://www.ginac.de/CLN/>.
- [49] M. Galassi, et al., *GNU Scientific Library: Reference Manual*, Network Theory Ltd., 2003.
- [50] J.F. Williams, *J. Phys. B: At. Mol. Phys.* 14 (1981) 1197.
- [51] G. Rixon, M.L. Dubernet, N. Piskunov, N. Walton, 7th International Conference on Atomic and Molecular Data and Their Applications – ICAMDATA-2010 AIP, Vol. 1344, Vilnius, Lithuania, 2011, pp. 107–115.
- [52] M. Frigo, Steven, G. Johnson, *Proceedings of the IEEE* 93 (2005) 216–231.
- [53] The HDF Group, *Hierarchical data format version 5 (2000–2014)*. <http://www.hdfgroup.org/HDF5>.